

KINETIC THEORY OF PLASMA WAVES: Part II Homogeneous Plasma*

E. Westerhof

FOM-Instituut voor Plasmafysica ‘Rijnhuizen’, Associatie Euratom-FOM,
Trilateral Euregio Cluster, PO Box 1207, 3430 BE Nieuwegein, The Netherlands

* This lecture is reprinted from the 4th and 5th Carolus Magnus Summer School proceedings with minor corrections.

ABSTRACT

The theory of electromagnetic waves in a homogeneous plasma is reviewed. The linear response of the plasma to the waves is obtained in the form of the dielectric tensor. Waves ranging from the low frequency Alfvén to the high frequency electron cyclotron waves are discussed in the limit of the cold plasma approximation. Bernstein waves are briefly treated as an example of waves in finite temperature plasmas.

I. INTRODUCTION

In the previous lecture the general framework for the theory of electromagnetic waves in plasmas has been set out [1]. This lecture treats the limit of homogeneous plasma. Tractable expressions are obtained that allow to explore the whole frequency domain. Starting point is the set of linearized Vlasov-Maxwell equations as discussed in the previous lecture (note the use of cgs units)

$$\frac{Df_{s1}}{Dt} = -q_s(\mathbf{E} + \frac{\mathbf{v}}{c} \times \mathbf{B}) \cdot \frac{\partial f_{s0}}{\partial \mathbf{p}}, \quad (1)$$

$$\nabla \times \mathbf{E} = -\frac{1}{c} \frac{\partial \mathbf{B}}{\partial t}, \quad \nabla \times \mathbf{B} = \frac{4\pi}{c} \mathbf{J} + \frac{1}{c} \frac{\partial \mathbf{E}}{\partial t}, \quad (2)$$

with the conditions

$$\nabla \cdot \mathbf{E} = 4\pi\rho, \quad \text{and} \quad \nabla \cdot \mathbf{B} = 0, \quad (3)$$

where the charge ρ and current density J are obtained from the first order perturbations of the distribution functions f_{s1} for all particle species s :

$$\rho = \sum_s q_s \int d^3\mathbf{p} f_{s1}(\mathbf{r}, \mathbf{p}, t), \quad (4)$$

$$\mathbf{J} = \sum_s q_s \int d^3\mathbf{p} \mathbf{v} f_{s1}(\mathbf{r}, \mathbf{p}, t). \quad (5)$$

Using the Fourier decomposition of the waves, the first order perturbation of the distribution functions f_{s1} is obtained and expressed in terms of the electric field of the wave. The first velocity moments of f_{s1} then give the plasma response to the wave in terms of the perturbed current density. This provides the conductivity

tensor σ and dielectric tensor $\epsilon = \mathbf{l} + (4\pi i/\omega)\sigma$, where \mathbf{l} is the identity matrix. Before proceeding to explicit expressions for ϵ in case of a thermal plasma, we briefly discuss the cyclotron resonances. Finally, the limit to vanishing plasma temperature, $T_s \rightarrow 0$, is taken. This ‘cold plasma’ approximation provides the basis for a short overview of plasma waves. The wave equation is obtained as usual from Maxwell’s equations using the dielectric tensor to quantify the plasma response:

$$\left(\mathbf{k}\mathbf{k} - k^2\mathbf{l} + \frac{\omega^2}{c^2}\epsilon \right) \cdot \mathbf{E} = \mathbf{A} \cdot \mathbf{E} = 0, \quad (6)$$

where \mathbf{A} is the dispersion tensor. The condition for nontrivial solutions of the wave equation is $\det\mathbf{A} = 0$, which provides the dispersion relation. The properties of the waves in the various frequency ranges will be briefly discussed. In the last part of this lecture, an example will be given of waves existing only in finite temperature plasma. More detail can be found in the textbooks [3, 4, 5].

Throughout this lecture, the z -axis is chosen along the equilibrium magnetic field and the perpendicular part of the wave vector is taken along the x -axis.

II. THE DIELECTRIC TENSOR

We remind here that the derivative D/Dt in the linearized Vlasov equation (1) symbolizes the total time derivative along unperturbed particle orbits of the equilibrium. Hence, a formal solution of (1) is obtained straightforwardly from the orbit integrals. In terms of the Fourier decomposition of the fields and the perturbed distribution function this gives for each of the particle species

$$f_{s,\mathbf{k},\omega}(\mathbf{p})e^{i\mathbf{k}\cdot\mathbf{r}-i\omega t} = -q_s \int_{-\infty}^t dt' e^{i\mathbf{k}\cdot\mathbf{r}'-i\omega t'} \left(\mathbf{E}_{\mathbf{k},\omega} + \frac{\mathbf{v}'}{c} \times \mathbf{B}_{\mathbf{k},\omega} \right) \cdot \frac{\partial f_{s0}}{\partial \mathbf{p}'}, \quad (7)$$

where the primes indicate the particle positions and velocities at the retarded time t' . The convergence of the

integrals requires the restriction to a vanishing perturbation and wave amplitudes at $t' \rightarrow -\infty$. This implies that the frequency ω is required to have a finite positive imaginary part. In case of a homogeneous plasma with the equilibrium magnetic field along \hat{z} , the particle position and momentum are

$$\begin{aligned} \mathbf{r}(t') - \mathbf{r}(t) &= v_{\parallel}(t' - t) \hat{z} \\ &+ \frac{p_{\perp}}{m_s \Omega_{cs}} \left[\sin(\phi + \omega_{cs}(t' - t)) - \sin \phi \right] \hat{x} \\ &+ \frac{p_{\perp}}{m_s \Omega_{cs}} \left[\cos(\phi + \omega_{cs}(t' - t)) - \cos \phi \right] \hat{y}, \end{aligned} \quad (8)$$

$$\begin{aligned} \mathbf{p}(t') &= p_{\parallel} \hat{z} + p_{\perp} \cos(\phi + \omega_{cs}(t' - t)) \hat{x} \\ &- p_{\perp} \sin(\phi + \omega_{cs}(t' - t)) \hat{y}, \end{aligned} \quad (9)$$

where parallel and perpendicular refer to the directions with respect to the equilibrium magnetic field, $\omega_{cs} = \Omega_{cs}/\gamma$ is the relativistic cyclotron frequency with $\Omega_{cs} \equiv q_s B_0 / m_s c$, and ϕ is the gyrophase at $t' = t$. *Note that, as defined here, the ion cyclotron frequencies are positive while the electron cyclotron frequency is negative.*

Next, the induction equation, $\mathbf{B}_{\mathbf{k},\omega} = \mathbf{N} \times \mathbf{E}_{\mathbf{k},\omega}$ is used to eliminate the fluctuating magnetic field (with the refractive index $\mathbf{N} \equiv \mathbf{k}c/\omega$); the time t' is substituted with $\tau = t - t'$, and a phase $\Phi(\tau)$ is defined

$$\Phi(\tau) \equiv (\omega - k_{\parallel} v_{\parallel})\tau + \frac{k_{\perp} p_{\perp}}{m_s \Omega_{cs}} \left[\sin(\phi - \omega_{cs}\tau) - \sin \phi \right]. \quad (10)$$

After some algebra taking into account that $f_{s0}(p_{\parallel}, p_{\perp})$, the perturbed distribution function is written

$$f_{s,\mathbf{k},\omega}(\mathbf{p}) = -q \int_0^{\infty} d\tau e^{i\Phi(\tau)} E_j. \quad (11)$$

$$\left[\frac{p'_j}{p_{\perp}} \left(\frac{\partial f_{s0}}{\partial p_{\perp}} + \frac{N_{\parallel}}{\gamma m_s c} F \right) + \delta_{zj} \frac{F}{p_{\perp}} \left(1 - \frac{\mathbf{p}' \cdot \mathbf{N}}{\gamma m_s c} \right) \right],$$

where F ,

$$F = p_{\perp} \frac{\partial f_{s0}}{\partial p_{\parallel}} - p_{\parallel} \frac{\partial f_{s0}}{\partial p_{\perp}}, \quad (12)$$

is a measure of the anisotropy of the equilibrium distribution function. Next, the Bessel function identities

$$e^{iz \sin \phi} \begin{cases} 1 \\ \sin \phi \\ \cos \phi \end{cases} = \sum_{n=-\infty}^{\infty} e^{in\phi} \begin{cases} J_n(z) \\ -i J'_n(z) \\ \frac{n}{z} J_n(z) \end{cases} \quad (13)$$

are used to expand part of the phase factor in a double infinite sum over cyclotron harmonics. The resulting perturbed distribution function is

$$\begin{aligned} f_{s,\mathbf{k},\omega}(\mathbf{p}) &= -q \int_0^{\infty} d\tau \sum_{n=-\infty}^{\infty} \sum_{m=-\infty}^{\infty} \\ &e^{i(\omega - k_{\parallel} v_{\parallel} - n\omega_{cs})\tau + i(n-m)\phi} J_m \begin{pmatrix} \frac{n}{b} J_n U \\ J'_n U \\ J_n W_n \end{pmatrix} \cdot \begin{pmatrix} E_x \\ E_y \\ E_z \end{pmatrix} \end{aligned} \quad (14)$$

where the quantities U and W_n are defined by

$$U \equiv \frac{\partial f_{s0}}{\partial p_{\perp}} + \frac{N_{\parallel}}{\gamma m_s c} F \quad W_n \equiv \frac{\partial f_{s0}}{\partial p_{\parallel}} - \frac{n\Omega_{cs}}{\omega \gamma p_{\perp}} F, \quad (15)$$

and with the Bessel functions of argument b ,

$$b \equiv \frac{k_{\perp} p_{\perp}}{m_s \Omega_{cs}} \quad (16)$$

which is a measure of the ration of the Larmor radius over the wave length. The time integration has now become trivial: for each n , one obtains

$$\int_0^{\infty} d\tau e^{i(\omega - k_{\parallel} v_{\parallel} - n\omega_{cs})\tau} = \frac{i}{\omega_+ - k_{\parallel} v_{\parallel} - n\omega_{cs}}, \quad (17)$$

where the subscript of ω_+ signifies the condition $\omega_i > 0$ as discussed above.

From the perturbed distribution function, the current induced by the waves is obtained as

$$\mathbf{J}_{\mathbf{k},\omega} = \sum_s q_s \int d^3p \mathbf{v} f_{s,\mathbf{k},\omega}(\mathbf{p}) = \boldsymbol{\sigma}(\mathbf{k},\omega) \cdot \mathbf{E}_{\mathbf{k},\omega}, \quad (18)$$

which allows to calculate the plasma conductivity tensor $\boldsymbol{\sigma}$. Note, that velocity and momentum are related by $v = p/(\gamma m_s)$, where $\gamma = 1/\sqrt{1 - v^2/c^2} = \sqrt{1 + p^2/m_s^2 c^2}$ is the relativistic mass increase. The gyrophase integrals are performed first and lead to a reduction of the sum over m :

$$\int_0^{2\pi} d\phi \sum_{m=-\infty}^{\infty} J_m e^{i(n-m)\phi} \begin{cases} 1 \\ \sin \phi \\ \cos \phi \end{cases} = 2\pi \begin{cases} J_n \\ +i J'_n \\ \frac{n}{b} J_n \end{cases}. \quad (19)$$

With the help of the relation

$$p_{\parallel} U - p_{\perp} W_n = -F \frac{\omega - k_{\parallel} v_{\parallel} - n\omega_{cs}}{\omega}$$

and the Bessel function identities $\sum_{n=-\infty}^{\infty} n J_n^2 = 0$, and $\sum_{n=-\infty}^{\infty} J_n J'_n = 0$, the conductivity tensor is finally obtained as

$$\boldsymbol{\sigma} = -i \sum_s \frac{\omega_{ps}^2}{4\pi} \sum_{n=-\infty}^{\infty} \int \frac{d^3p}{\gamma n_s} \frac{\mathbf{S}_n}{\omega_+ - k_{\parallel} v_{\parallel} - n\omega_{cs}} \quad (20)$$

with the tensors \mathbf{S}_n in Hermitian form

$$\mathbf{S}_n = \begin{pmatrix} \frac{n^2}{b^2} J_n^2 p_{\perp} U & +i \frac{n}{b} J_n J'_n p_{\perp} U & \frac{n}{b} J_n^2 p_{\parallel} U \\ -i \frac{n}{b} J_n J'_n p_{\perp} U & J'_n J'_n p_{\perp} U & -i J_n J'_n p_{\parallel} U \\ \frac{n}{b} J_n^2 p_{\parallel} U & +i J_n J'_n p_{\parallel} U & J_n^2 p_{\parallel} W_n \end{pmatrix}.$$

Here, the $\omega_{ps} \equiv (4\pi n_s q_s^2 / m_s)^{\frac{1}{2}}$ are the plasma frequencies for the different species. In case of an isotropic

distribution function $f_{s0}(p)$ with $F = 0$, the conductivity tensor is further simplified to

$$\boldsymbol{\sigma} = -i \sum_s \frac{\omega_{ps}^2}{4\pi} \sum_{n=-\infty}^{\infty} \int \frac{d^3p}{\gamma n_s \omega_+ - k_{\parallel} v_{\parallel} - n\omega_{cs}} \frac{1}{p} \frac{\partial f_{s0}}{\partial p} \boldsymbol{\Pi}_n \quad (21)$$

with

$$\boldsymbol{\Pi}_n = \begin{pmatrix} \frac{n^2}{b^2} J_n^2 p_{\perp}^2 & +i \frac{n}{b} J_n J_n' p_{\perp}^2 & \frac{n}{b} J_n^2 p_{\perp} p_{\parallel} \\ -i \frac{n}{b} J_n J_n' p_{\perp}^2 & J_n J_n' p_{\perp}^2 & -i J_n J_n' p_{\perp} p_{\parallel} \\ \frac{n}{b} J_n^2 p_{\perp} p_{\parallel} & +i J_n J_n' p_{\perp} p_{\parallel} & J_n^2 p_{\parallel}^2 \end{pmatrix}.$$

These expressions are generalized to frequencies with arbitrary imaginary part by analytic continuation. The result is known as the Landau contour for integration is written symbolically as

$$\frac{1}{\omega - k_{\parallel} v_{\parallel} - n\omega_{cs}} = \mathcal{P} \frac{1}{\omega - k_{\parallel} v_{\parallel} - n\omega_{cs}} - \nu i \pi \delta(\omega - k_{\parallel} v_{\parallel} - n\omega_{cs}), \quad (22)$$

where \mathcal{P} indicates the principal value integral, while $\nu = 0, 1, 2$ for frequencies with positive, zero, and negative imaginary part, respectively.

A. Cyclotron Resonance

The resonant wave-particle interaction that occurs for the Landau $n = 0$ and cyclotron $n \neq 0$ resonances,

$$\omega - k_{\parallel} v_{\parallel} - n\omega_{cs} = 0, \quad (23)$$

determines the wave damping or growth. It is thus of interest to analyze which particles satisfy the resonance condition. Note that, because the electron cyclotron frequency is negative by definition, the fundamental electron cyclotron resonance occurs for $n = -1$ and the harmonic electron cyclotron resonances for $n \leq -2$. Without approximation we can write the solution in terms of the parallel and perpendicular momenta in the form

$$\frac{n^2 \Omega_{cs}^2}{\omega^2 (1 - N_{\parallel}^2)} - 1 = (1 - N_{\parallel}^2) \left(\frac{p_{\parallel}}{m_s c} - \frac{n N_{\parallel} \Omega_{cs}}{\omega (1 - N_{\parallel}^2)} \right)^2 + \left(\frac{p_{\perp}}{m_s c} \right)^2. \quad (24)$$

For $N_{\parallel} < 1$ this is the equation for an ellipse and for $N_{\parallel} > 1$ it designates a hyperbola. It is important to note here, that for $N_{\parallel} < 1$ resonant interaction is impossible for $\omega > n\Omega_{cs}/(1 - N_{\parallel}^2)^{\frac{1}{2}}$, which excludes anomalous cyclotron resonance $n\Omega_{cs} < 0$ entirely.

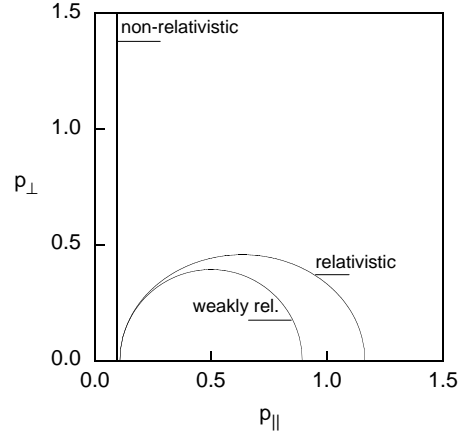


Figure 1: The resonance condition according to the different approximations with $\omega/\Omega_{ce} = -1.05$ and $N_{\parallel} = 0.5$, as might occur in experimental applications of EC waves. Up to fairly high momenta the weakly relativistic approximation gives reasonable results. The non-relativistic approximation is clearly inapplicable for these parameters.

To obtain simpler and analytically more tractable expressions, one often employs the non-relativistic approximation, which is obtained by setting $\gamma = 1$ in the cyclotron resonance condition (23). This results in the condition

$$N_{\parallel} \frac{p_{\parallel}}{m_s c} = 1 - \frac{n\Omega_{cs}}{\omega}, \quad (25)$$

which represents a straight line at constant p_{\parallel} in momentum space. The validity of this approximation requires that both $|N_{\parallel}| \gg v_t/c$, where v_t is a typical resonant or thermal velocity, and $|N_{\parallel}| \gg |1 - n\Omega_{cs}/\omega|$. These conditions guarantee that the Doppler effect dominates the relativistic cyclotron frequency downshift and that resonant velocities remain subrelativistic. Though these conditions generally apply in case of laboratory applications of ion cyclotron waves, they are generally not valid in case of electron cyclotron wave applications.

When the non-relativistic approximation breaks down, a useful and often used approximation is the weakly relativistic one, setting $\gamma \approx 1 + \frac{1}{2} p^2/m_s^2 c^2$ in the resonance condition. The resonance curve, valid for all N_{\parallel} , is then given by a circle

$$\left(\frac{p_{\parallel}}{m_s c} - N_{\parallel} \right)^2 + \left(\frac{p_{\perp}}{m_s c} \right)^2 = 2 \left(\frac{n\Omega_{cs}}{\omega} - 1 + \frac{1}{2} N_{\parallel}^2 \right). \quad (26)$$

Resonant interaction is now excluded for frequencies $\omega > n\Omega_{cs}/(1 - \frac{1}{2} N_{\parallel}^2)$. For the wave parameters typical of applications of electron cyclotron waves, this approximation provides satisfactory results for temperatures up to $T_e = 10$ keV.

B. Thermal Plasma Dielectric Tensor

In most cases the equilibrium particle distribution functions are Maxwellian,

$$f_{s0} = \frac{n_s e^{-\mu_s \gamma}}{4\pi m_s^3 c^3 K_2(\mu_s)} \approx \frac{n_s e^{-\frac{1}{2} p^2 / m_s k_B T_s}}{(2\pi m_s k_B T_s)^{3/2}}, \quad (27)$$

where $\mu_s \equiv m_s c^2 / k_B T_s$ and the first expression gives the relativistic Maxwellian and the second its non- or weakly relativistic approximation. The dielectric tensor for a thermal plasma is obtained by substitution of Maxwellian distribution functions in Eq. (21). The relativistic dielectric tensor can only be obtained from numerical calculations. In case of the non- and weakly relativistic approximations analytical expressions have been obtained. For the purpose of illustration, the non-relativistic results are summarized here. In the non-relativistic approximation, the relativistic downshift of the cyclotron frequency is neglected. The resonant denominator then depends only on the parallel momentum. The parallel momentum integrals can be expressed in terms of the plasma dispersion function Z , defined below, while the perpendicular momentum integrals take the form of modified Bessel functions I_n . The final result is

$$\epsilon^{\text{thermal}} = 1 + \sum_s \frac{\omega_{ps}^2}{\omega^2} \frac{c}{\sqrt{2} N_{\parallel} v_{ts}} \sum_{n=-\infty}^{\infty} \mathbf{E}_n, \quad (28)$$

with

$$\mathbf{E}_n = \begin{pmatrix} \frac{n^2}{\lambda} \Gamma Z & +in\Gamma' Z & \sqrt{\frac{2}{\lambda}} n \zeta_n \Gamma Z \\ -in\Gamma' Z & \left(\frac{n^2}{\lambda} \Gamma - 2\lambda\Gamma' \right) Z & -i\zeta_n \sqrt{2\lambda} \Gamma' Z \\ \sqrt{\frac{2}{\lambda}} n \zeta_n \Gamma Z & +i\zeta_n \sqrt{2\lambda} \Gamma' Z & 2\zeta_n \Gamma(1 + \zeta_n Z) \end{pmatrix}$$

where $\Gamma = \Gamma_n(\lambda) = e^{-\lambda} I_n(\lambda)$ with the argument $\lambda = k_{\perp}^2 v_{ts}^2 / \Omega_{cs}^2$ and where the prime denotes a differentiation with respect to the argument. The thermal velocity is defined as $v_{ts} = (k_B T_s / m_s)^{1/2}$. The argument of the plasma dispersion function Z is

$$Z(\zeta_n) \quad \text{with} \quad \zeta_n = \frac{\omega - n\Omega_{cs}}{\sqrt{2} k_{\parallel} v_{ts}} \quad (29)$$

Finally, it is noted that the square root of λ has to be interpreted algebraically, i.e. $\sqrt{\lambda} = k_{\perp} v_{ts} / \Omega_{cs}$ with the sign of $\sqrt{\lambda}$ thus depending on the sign of Ω_{cs} .

The quantity λ is a measure of the squared ratio of the Larmor radius of a thermal particle and the wave length. It is a measure of the importance of finite gyro-radius effects. In the limits of small ($\lambda \ll 1$) and large ($\lambda \gg 1$) Larmor radii one may use

$$e^{-\lambda} I_n(\lambda) \approx \begin{cases} \frac{1}{|n|!} \frac{\lambda^{|n|}}{2^{|n|}} & \text{for } \lambda \ll 1 \\ \frac{1}{\sqrt{2\pi\lambda}} & \text{for } \lambda \gg 1. \end{cases} \quad (30)$$

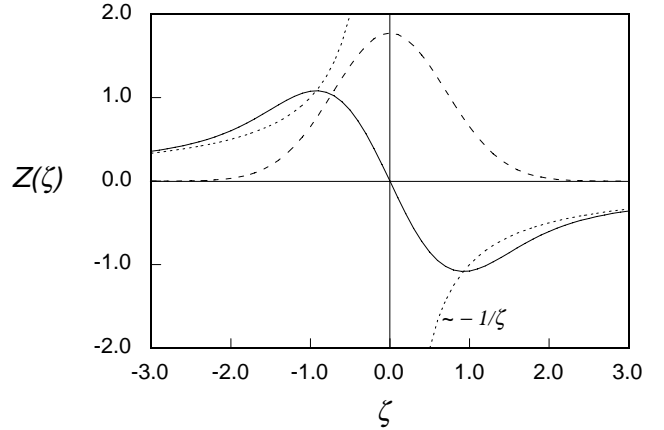


Figure 2: Real (full curve) and imaginary (dashed curve) parts of the plasma dispersion function $Z(\zeta)$.

The expression for small Larmor radii corresponds to the first term of the series expansion of the modified Bessel functions. Such an approximation is often referred to as lowest order finite Larmor radius (FLR) approximation.

Intermezzo: the plasma dispersion function Z

Here, only the definition and a limited number of important properties of the plasma dispersion function are provided. A detailed discussion is given by Fried and Conte [2]. The definition is

$$Z(\zeta) \equiv \frac{1}{\sqrt{\pi}} \int dx \frac{e^{-x^2}}{x - \zeta}, \quad (31)$$

for complex arguments with $\text{Im} \zeta > 0$ and as the analytic continuation for $\text{Im} \zeta \leq 0$. An alternative representation, valid over the entire complex plane, is

$$Z(\zeta) = 2ie^{-\zeta^2} \int_{-\infty}^{i\zeta} dt e^{-t^2}. \quad (32)$$

The latter shows that the plasma dispersion function is related to the (complex) error function.

Mostly, the plasma dispersion function has to be evaluated numerically, but in the limits of small ζ or of large ζ the following power series or asymptotic expansion, respectively, are useful:

a) power series [2]

$$Z(\zeta) = i\sqrt{\pi}e^{-\zeta^2} - \sum_{n=0}^{\infty} \frac{(-1)^n 2(n+1)}{(2n+1)!!} \zeta^{2n+1} \quad (33)$$

$$\approx i\sqrt{\pi}e^{-\zeta^2} - 2\zeta[1 - 2\zeta^2/3 + 4\zeta^4/15 - \dots],$$

b) asymptotic expansion for large ζ [2]

$$Z(\zeta) = i\sqrt{\pi}e^{-\zeta^2} - \sum_{n=0}^{\infty} \frac{(2n-1)!!}{2^n} \zeta^{-(2n+1)} \quad (34)$$

$$\approx i\sqrt{\pi}e^{-\zeta^2} - \zeta^{-1}[1 + 1/2\zeta^2 + 3/4\zeta^4 + \dots].$$

C. The Cold Plasma Approximation

In order to be able to present a global overview of plasma waves on the basis of a tractable dispersion relation, we discuss here one further approximation. That is the cold plasma approximation in which the limit $v_{ts} \rightarrow 0$ is taken. This means that we can use the small argument expansion (30) for the functions $\Gamma_n(\lambda)$. The contributions from the different cyclotron harmonic terms to the dielectric tensor elements ε_{ij} with $i = 1, 2$ and $j = 1, 2$ then are of order $|n|v_{ts}^{2(|n|-1)}$, such that only the $n = \pm 1$ terms give a finite contribution. For the parallel element of the dielectric tensor ε_{33} the contributions are of order $v_{ts}^{2|n|}$, and only the $n = 0$ or Landau resonance term will give a finite contribution. In the remaining elements the contributions are of order $|n|v_{ts}^{2|n|-1}$, and none provides a finite contribution. The plasma dispersion function is approximated by its large argument expansion (34), and in the limit of zero temperatures the imaginary part of the plasma dispersion function reduces to a delta function. As a result the cold plasma dielectric tensor elements become

$$\begin{aligned} \varepsilon_{11} = \varepsilon_{22} = 1 - \sum_s \frac{\omega_{ps}^2}{2\omega} \left(\frac{1}{\omega + \Omega_{cs}} + i\pi\delta(\omega + \Omega_{cs}) \right) \\ - \sum_s \frac{\omega_{ps}^2}{2\omega} \left(\frac{1}{\omega - \Omega_{cs}} + i\pi\delta(\omega - \Omega_{cs}) \right) \end{aligned} \quad (35)$$

$$\begin{aligned} \varepsilon_{12} = -\varepsilon_{21} = +i \sum_s \frac{\omega_{ps}^2}{2\omega} \left(\frac{1}{\omega + \Omega_{cs}} + i\pi\delta(\omega + \Omega_{cs}) \right) \\ - i \sum_s \frac{\omega_{ps}^2}{2\omega} \left(\frac{1}{\omega - \Omega_{cs}} + i\pi\delta(\omega - \Omega_{cs}) \right) \end{aligned} \quad (36)$$

$$\varepsilon_{33} = 1 - \sum_s \frac{\omega_{ps}^2}{\omega} \left(\frac{1}{\omega} + i\pi\delta(\omega) \right), \quad (37)$$

with the remaining elements being equal to zero.

The delta functions are a consequence of causality and are required for the dielectric tensor to satisfy Kramers-Kronig relations (see e.g. [3]). In the following the delta functions are taken as implicit in the resonant denominators, and the cold plasma dielectric tensor is written in the convenient form

$$\boldsymbol{\varepsilon}^{\text{cold}} = \begin{pmatrix} S & -iD & 0 \\ +iD & S & 0 \\ 0 & 0 & P \end{pmatrix}, \quad (38)$$

where

$$S \equiv \frac{1}{2}(R + L) = 1 - \sum_s \frac{\omega_{ps}^2}{\omega^2 - \Omega_{cs}^2}, \quad (39)$$

$$D \equiv \frac{1}{2}(R - L) = \sum_s \frac{\Omega_{cs}\omega_{ps}^2}{\omega(\omega^2 - \Omega_{cs}^2)}, \quad (40)$$

$$P \equiv 1 - \sum_s \frac{\omega_{ps}^2}{\omega^2}, \quad (41)$$

with

$$R \equiv 1 - \sum_s \frac{\omega_{ps}^2}{\omega(\omega + \Omega_{cs})}, \quad (42)$$

$$L \equiv 1 - \sum_s \frac{\omega_{ps}^2}{\omega(\omega - \Omega_{cs})}, \quad (43)$$

The identical dielectric tensor would also be obtained from a multi-fluid plasma model neglecting the pressures and collisions.

III. AN OVERVIEW OF COLD PLASMA WAVES

In this section, an overview is given of cold plasma waves covering the whole range of frequencies from the low frequency Alfvén waves to the high frequencies around the electron cyclotron resonance and well above. The emphasis will be on the waves as they are applied or observed for heating and or diagnostic purposes in tokamak plasmas.

With the cold dielectric tensor as given by Eq. (38) the dispersion tensor $\mathbf{\Lambda}$ becomes

$$\mathbf{\Lambda} = \frac{\omega^2}{c^2} \begin{pmatrix} S - N^2 \cos^2 \theta & -iD & N^2 \cos \theta \sin \theta \\ iD & S - N^2 & 0 \\ N^2 \cos \theta \sin \theta & 0 & P - N^2 \sin^2 \theta \end{pmatrix}, \quad (44)$$

where θ is the angle of the wave vector with respect to the equilibrium magnetic field. From the dispersion tensor the dispersion relation is derived straightforwardly as $\det \mathbf{\Lambda} = 0$. A common representation of the dispersion relation takes the form of a bi-quadratic equation for the wave refractive index N

$$AN^4 - BN^2 + C = 0, \quad (45)$$

with

$$\begin{aligned} A &\equiv S \sin^2 \theta + P \cos^2 \theta, \\ B &\equiv RL \sin^2 \theta + PS(1 + \cos^2 \theta), \\ C &\equiv PRL. \end{aligned} \quad (46)$$

The dispersion relation is considerably simplified for the cases of parallel propagation, $\theta = 0$ with the solutions

$$N^2 = R, \quad N^2 = L, \quad \text{or} \quad P = 0, \quad (47)$$

and of perpendicular propagation, $\theta = \frac{\pi}{2}$ with the solutions

$$N^2 = \frac{RL}{S} \quad \text{or} \quad N^2 = P. \quad (48)$$

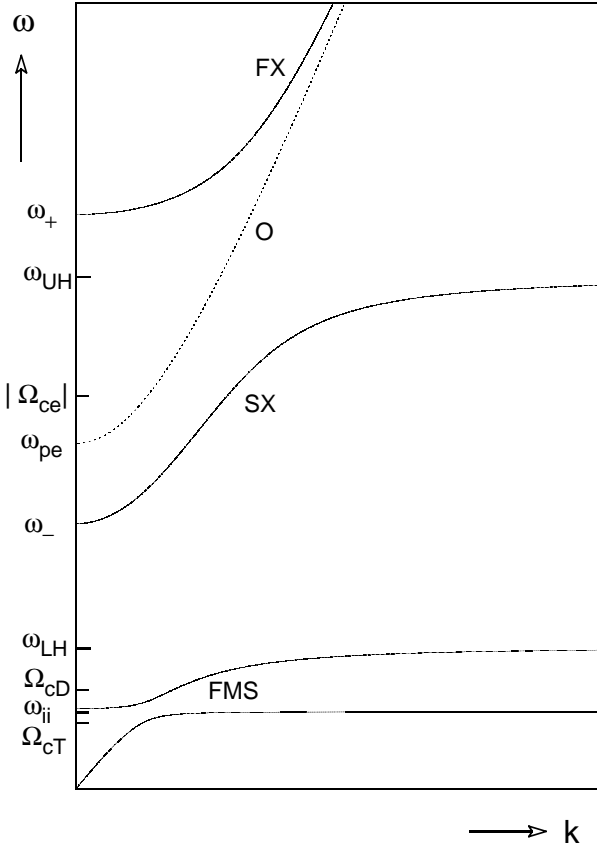


Figure 3: The dispersion diagram for the case of perpendicular propagation. Solid lines refer to the different branches of the X-mode and the dotted line to the O-mode.

The latter two solutions are known as the extraordinary or X-mode and ordinary or O-mode, respectively.

An important role in dispersion and wave propagation is played by the wave cut-off's and wave resonances. A wave cut-off is the position or frequency at which the refractive index vanishes, i.e. $N^2 = 0$. The condition for a wave cut-off is $C = 0$ which means

$$P = 0, \quad R = 0, \quad \text{or} \quad L = 0. \quad (49)$$

Neglecting the ion contributions, the corresponding cut-off frequencies are

$$\omega_{pe}, \quad \text{and} \quad \omega_{\pm} = \pm \frac{1}{2} |\Omega_{ce}| + \sqrt{\left(\frac{1}{2} \Omega_{ce}\right)^2 + \omega_{pe}^2} \quad (50)$$

A wave resonance is said to occur when the wave refractive index becomes infinite, i.e. $N^2 = \infty$. The condition for a wave resonance is $A = 0$, which can be written as a condition on the angle θ as $\tan^2 \theta = -P/S$. For parallel propagating waves, $\theta = 0$, the condition becomes

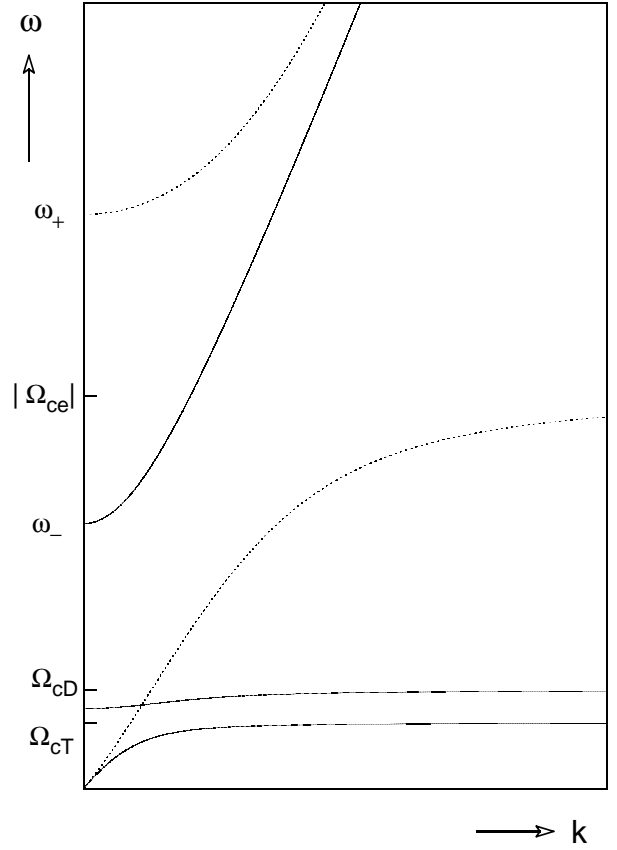


Figure 4: The dispersion diagram for the case of parallel propagation. Solid lines refer to the different branches of the L-mode and the dotted lines to the R-mode branches.

$S = \frac{1}{2}(R + L) = \pm\infty$ and wave resonances are seen to occur at the cyclotron frequencies $|\Omega_{cs}|$. For perpendicular propagation one has the hybrid resonances, which occur at $S = 0$. One hybrid resonance is found above each of the cyclotron frequencies of the various particle species. The wave resonance found above the electron cyclotron frequency is known as the Upper Hybrid (UH) resonance with

$$\omega_{UH} \equiv \sqrt{\Omega_{ce}^2 + \omega_{pe}^2} \quad (51)$$

In between the electron and ion cyclotron frequencies one has the Lower Hybrid (LH) resonance with

$$\omega_{LH}^2 = \frac{\omega_{pi}^2}{1 + \omega_{pe}^2/\Omega_{ce}^2} = \frac{\Omega_{ci}|\Omega_{ce}|}{1 + \Omega_{ce}^2/\omega_{pe}^2}. \quad (52)$$

In between the various ion cyclotron frequencies wave resonances occur: the ion-ion hybrid resonances. With each ion-ion hybrid resonance a cut-off is associated.

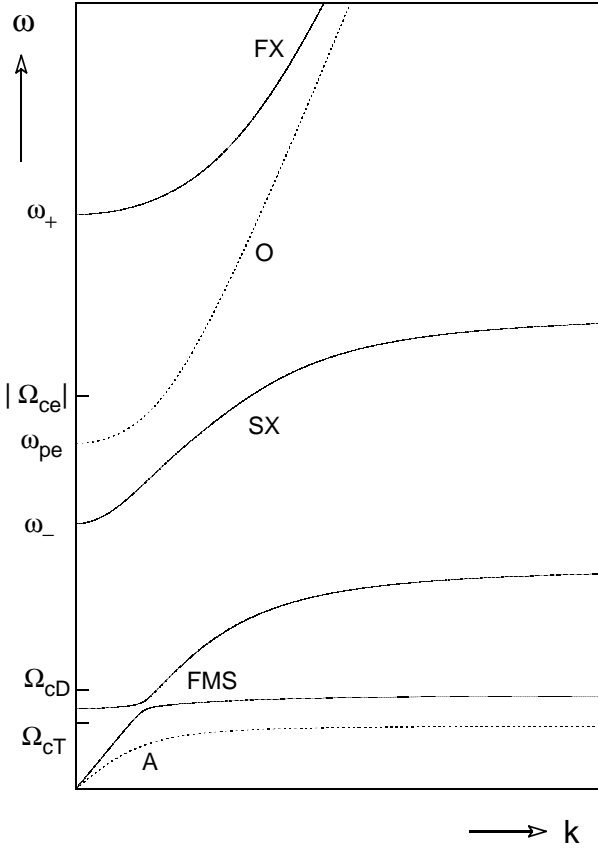


Figure 5: The solutions of the cold plasma dispersion relation for the case of oblique propagation. In addition to the X- and O-mode branches found for perpendicular propagation, the low frequency Alfvén branch is seen.

Examples of the wave dispersion diagrams for perpendicular, parallel and oblique propagation are presented in Fig's 3 to 5, respectively. These figures refer to a plasma with a 50%/50% mix of Deuterium and Tritium ions. For perpendicular propagation a single O-mode branch is found. The X-mode is split in different branches by the hybrid resonances. The high frequency branch is known as the fast extraordinary (FX) mode and the intermediate branch as the slow extraordinary (SX) mode. The low frequency branch is identified as the fast magnetosonic (FMS) mode. Note, that the latter is split by the DT ion-ion hybrid resonance.

For oblique propagation one recognizes the wave branches as defined for perpendicular propagation. Additionally, the low frequency shear Alfvén wave is found, which is limited from above by the Alfvén resonance.

Due to the toroidal symmetry and predominantly toroidal magnetic field of a tokamak the parallel wave refractive index N_{\parallel} is approximately conserved as a

wave propagates into a tokamak. In order to assess wave penetration in a tokamak it is thus instructive to write the dispersion relation in terms of N_{\perp} with constant N_{\parallel} . Again a bi-quadratic equation is obtained

$$A' N_{\perp}^4 - B' N_{\perp}^2 + C' = 0, \quad (53)$$

with coefficients

$$A' \equiv S, \quad B' \equiv (S + P)(S - N_{\parallel}^2) - D^2, \quad (54)$$

$$C' \equiv P(R - N_{\parallel}^2)(L - N_{\parallel}^2) = P((S - N_{\parallel}^2)^2 - D^2).$$

One observes that the wave resonances, $N_{\perp} \rightarrow \infty$, are identical to those for perpendicular propagation, i.e. $S = 0$. From the cut-off's $N_{\perp} = 0$, only the O-mode cut-off, $P = 0$, is unaltered while the X-mode cut-off's are altered to

$$\omega_{\pm} = \pm \frac{1}{2} |\Omega_{ce}| + \sqrt{\left(\frac{1}{2} \Omega_{ce}\right)^2 + \omega_{pe}^2 / (1 - N_{\parallel}^2)}. \quad (55)$$

Qualitatively, the dispersion diagrams will thus be very similar to the dispersion diagrams for perpendicular propagation (for example, Fig. 3). Only the cut-off ω_{-} might occur at frequencies equal to or above ω_{pe} , in which case ω_{-} becomes the O-mode and ω_{pe} becomes the slow extraordinary mode cut-off.

Note, that the wave refractive index can be strongly dependent on the angle of the wave vector with respect to the magnetic field. This has important consequences for the wave propagation: the direction of propagation, $\mathbf{v}_g = \partial\omega/\partial\mathbf{k}$, is not simply parallel to the wave vector, but is perpendicular to the surface spanned by the wave vectors. The latter is known as the wave vector surface. Especially near wave resonances in a tokamak $N_{\perp} \rightarrow \infty$ this means that wave propagation will become parallel to the magnetic field. Thus, wave energy accumulates near a resonance, and wave-particle interaction will be strongly localized there.

A. Low frequencies: Alfvén waves

Here, a closer look is taken at the lowest frequency waves, $\omega \ll \omega_{ps}, |\Omega_{cs}|$. For those frequencies the dispersion relation is considerably simplified. Neglecting terms of order $\omega/|\Omega_{cs}|$ the different quantities in the cold plasma dispersion tensor are approximated as

$$R \approx L \approx S \approx 1 + \frac{4\pi\rho c^2}{B^2} = 1 + \frac{c^2}{c_A^2} \quad \text{and} \quad D \approx 0, \quad (56)$$

where ρ is the total mass density and $c_A \equiv \sqrt{B^2/4\pi\rho}$ is the Alfvén velocity. Furthermore, P will be very much larger than S , and the coefficients of the bi-quadratic dispersion relation (45) can be approximated by

$$A \approx -\frac{\omega_{pe}^2}{\omega^2} \cos^2 \theta,$$

$$B \approx -\frac{\omega_{pe}^2}{\omega^2} \left(1 + \frac{c^2}{c_A^2}\right) (1 + \cos^2 \theta), \quad (57)$$

$$C \approx -\frac{\omega_{pe}^2}{\omega^2} \left(1 + \frac{c^2}{c_A^2}\right)^2.$$

With these approximations the resulting bi-quadratic equation can be factorized as

$$\left[N_{\parallel}^2 - \left(1 + \frac{c^2}{c_A^2}\right)\right] \left[N^2 - \left(1 + \frac{c^2}{c_A^2}\right)\right] = 0. \quad (58)$$

which yields the dispersion relations

$$\omega^2 \approx k_{\parallel}^2 c_A^2 \quad \text{and} \quad \omega^2 \approx k^2 c_A^2 \quad (59)$$

for the shear Alfvén (the low frequency dotted curve in Fig. 5) and fast compressional Alfvén (or fast magnetosonic) waves, respectively. Note, that the shear Alfvén wave frequency is independent of the perpendicular wave vector and, consequently, shear Alfvén waves propagate exactly parallel to the magnetic field. The fast compressional Alfvén wave is modified significantly by finite pressure effects. The latter also yield an additional wave branch, the slow compressional Alfvén (or ion acoustic) waves. For more details see the lectures by H. Goedbloed [6].

In a plasma with closed magnetic fields as in a tokamak the shear Alfvén wave is confined within a magnetic surface, and direct excitation by an external antenna is impossible. When a compressional Alfvén wave is excited externally with frequency ω_d and wave vector \mathbf{k}_d , it propagates until it reaches a position where wave frequency and vector match the local shear Alfvén wave resonance, $\omega_d = k_{d\parallel} c_A$. There, the wave is converted to the shear Alfvén branch and energy accumulates. This process is halted by wave damping due to dissipative effects like finite resistivity or viscosity not included in the present model.

B. Ion Cyclotron (IC) Range of Frequencies

Next, we look at the waves in the ion cyclotron range of frequencies. Note, that except for exactly parallel propagation there are no wave resonances at the ion cyclotron frequencies, in spite of the infinite contributions from individual dielectric tensor elements. The reason is that in the cold plasma approximation the wave attains a right-handed circular polarization at the resonance, opposite to the ion-gyromotion. Consequently, in the cold plasma approximation no wave damping occurs at the cyclotron resonance. Cyclotron resonant absorption is essentially a finite Larmor radius, warm plasma effect. When the polarization is determined by the majority ion species, efficient damping at the fundamental resonance of a minority ion species is possible.

In the finite density interior of tokamaks, the dispersion relation for N_{\perp}^2 is considerably simplified by

noting that ω_{pe}^2/ω^2 is very much larger than other quantities occurring in the dispersion relation such that the coefficients may be approximated as

$$A' = S, \quad B' \approx -(\omega_{pe}^2/\omega^2)(S - N_{\parallel}^2),$$

$$C' \approx -(\omega_{pe}^2/\omega^2)((S - N_{\parallel}^2)^2 - D^2). \quad (60)$$

The two solutions of the dispersion relation then may be approximated by

$$N_{\perp}^2 \approx \frac{C'}{B'} = \frac{(S - N_{\parallel}^2)^2 - D^2}{(S - N_{\parallel}^2)}, \quad (61)$$

which is the continuation of the fast compressional Alfvén wave and the slow wave solution

$$N_{\perp}^2 \approx \frac{B'}{A'} = -\frac{\omega_{pe}^2}{\omega^2} \frac{(S - N_{\parallel}^2)}{S} \approx -\frac{\omega_{pe}^2}{\omega^2}. \quad (62)$$

The latter solution is seen to be highly evanescent in the plasma interior. Consequently, for wave-particle interaction at the ion cyclotron frequencies the fast wave is applied. In a multi-species plasma, ion-ion hybrid resonances occur on the fast wave branch between the various ion cyclotron frequencies. When the ion-ion hybrid resonance occurs close to a minority cyclotron resonance, wave energy accumulates there, and damping on the minority ion species can become particularly effective. Also conversion to warm plasma ion-Bernstein waves can occur at a hybrid resonance.

Vacuum wavelengths for frequencies in the ion cyclotron range are several meters, i.e. comparable with the size of tokamak devices. Consequently, antenna structures at the plasma edge typically generate waves with high values of $N_{\parallel} > 1$ which do not propagate in vacuum and must be coupled to waves existing in the finite density plasma edge. This problem of wave coupling is treated in a separate lecture [7]. Further details on heating and current drive by ion cyclotron waves are given in [8].

C. Lower Hybrid (LH) Range of Frequencies

In this range of frequencies, $\Omega_{ci} \ll \omega \ll |\Omega_{ce}|$, and the dielectric tensor elements are well approximated as

$$S \approx 1 - \frac{\omega_{pi}^2}{\omega^2} + \frac{\omega_{pe}^2}{\Omega_{ce}^2} \quad D \approx \frac{\omega_{pe}^2}{\omega \Omega_{ce}} \quad P \approx -\frac{\omega_{pe}^2}{\omega^2}, \quad (63)$$

such that the coefficients of the bi-quadratic dispersion relation for N_{\perp}^2 become

$$A' = 1 - \frac{\omega_{pi}^2}{\omega^2} + \frac{\omega_{pe}^2}{\Omega_{ce}^2},$$

$$B' \approx -\frac{\omega_{pe}^2}{\omega^2} \left(1 - N_{\parallel}^2 - \frac{\omega_{pi}^2}{\omega^2} + \frac{2\omega_{pe}^2}{\Omega_{ce}^2}\right), \quad (64)$$

$$C' \approx -\frac{\omega_{pe}^6}{\omega^4 \Omega_{ce}^2}.$$

The mode of interest now is the slow wave, exhibiting the lower hybrid resonance. An analysis of wave dispersion near the plasma edge shows that a condition for slow wave propagation is [5]:

$$N_{\parallel}^2 > N_c^2 = \frac{1}{1 - \omega^2/|\Omega_{ci}\Omega_{ce}|} \quad (65)$$

The slow wave dispersion relation is $N_{\perp}^2 \approx B'/A'$, which for sufficiently large N_{\parallel} , such that $B' \approx N_{\parallel}^2(\omega_{pe}^2/\omega^2)$, can be approximated by

$$N_{\perp}^2 = N_{\parallel}^2 \frac{\omega_{pe}^2}{\omega^2} \left(1 - \frac{\omega_{pi}^2}{\omega^2} + \frac{\omega_{pe}^2}{\Omega_{ce}^2} \right)^{-1}. \quad (66)$$

Thus, the direction of the wave vector is independent of its amplitude. A straightforward calculation gives the group velocity as

$$v_{g\parallel} = \frac{\partial\omega}{\partial k_{\parallel}} = \frac{1}{k_{\parallel}} \frac{\omega^2 - \omega_{LH}^2}{\omega} \quad (67)$$

$$v_{g\perp} = \frac{\partial\omega}{\partial k_{\perp}} = \frac{-1}{k_{\perp}} \frac{\omega^2 - \omega_{LH}^2}{\omega} \quad (68)$$

which is perpendicular to the wave vector. The direction of propagation is independent of the parallel refractive index. When a spectrum of waves is excited at some position in the plasma, the waves do not diverge but propagate on a so-called resonance cone. Since for LH waves $N_{\perp} \gg N_{\parallel}$, this resonance cone is narrow and directed almost parallel to the magnetic field.

Damping of LH waves can occur by interaction with both electrons and ions. Since $|N_{\parallel}| > 1$ efficient Landau damping is possible on the electrons and significant high velocity tails can be created on the electron distribution function. When the waves are excited with an asymmetric spectrum in N_{\parallel} , the electron tail will be in one direction and carry a significant amount of current [9]. At high densities damping is predominantly on the ions, and is a consequence of nonlinear interactions at high harmonic ion cyclotron resonances (see e.g. [5]).

D. Electron Cyclotron (EC) Range of Frequencies

As can be seen from Figs. 3 and 5 there are two modes propagating in the electron cyclotron range of frequencies: the ordinary (O) and extraordinary (X) mode. The latter is split in two branches by the upper hybrid resonance. Injection of waves in this frequency range is straightforward as all modes can directly propagate from vacuum into the plasma. O-mode waves injected from any position at the edge can propagate to the plasma interior provided $\omega > \omega_{pe}$. Thus, as long as $\omega_{pe}/|\Omega_{ce}| < 1$ in the plasma centre, O-mode waves can penetrate to the cyclotron resonance and will be efficiently damped there.

X-mode waves injected with $\omega > |\Omega_{ce}|$ at the plasma edge will be on the FX branch, while those injected with $\omega < |\Omega_{ce}|$ will be on the SX branch. Clearly waves on the FX branch will always encounter the ω_+ cut-off (55) before reaching the cyclotron resonance. Using higher frequencies the second harmonic EC resonance can be reached on the FX branch. Waves injected on the SX branch from the high field side of the tokamak can reach the cyclotron resonance provided the frequency remains above the SX cut-off, $\omega > \omega_-$ (55). Efficient absorption occurs both at fundamental and second harmonic EC resonance. In both cases the condition for the frequency to remain above cut-off yields $\omega_{pe}/|\Omega_{ce}| < \sqrt{2}$. For more on EC heating and current drive see [10].

For heating of high density plasmas, $\omega_{pe}/|\Omega_{ce}| > \sqrt{2}$ a scheme has been proposed using O-X-B conversion [11]. The O-mode cut-off $\omega = \omega_{pe}$ and the SX cut-off $\omega = \omega_-$ (55) coincide for the critical injection angle $N_{\parallel c}^2 = |\Omega_{ce}/\omega|/(1+|\Omega_{ce}/\omega|)$. For those conditions O- to X-mode conversion can occur at the cut-off. Subsequently, the X-mode will propagate backwards to the upper hybrid resonance where it is converted to electron Bernstein waves (see next Section). Finally, the Bernstein modes can propagate to the resonance and will be efficiently damped there. This scheme has been successfully employed on W7-AS [12].

IV. AN EXAMPLE OF WARM PLASMA WAVES: BERNSTEIN WAVES

The hot plasma dielectric response gives rise to waves that do not appear in cold plasma theory. In particular, a class of nearly perpendicularly propagating electrostatic waves has been found by I. Bernstein related to the cyclotron harmonic resonances. For nearly perpendicular propagation, the electrostatic dispersion relation is approximated by

$$\epsilon_{xx} = 0. \quad (69)$$

The non-relativistic dielectric tensor for a Maxwellian plasma Eq.(28) is now used, and the limit of $k_{\parallel} \rightarrow 0$ is taken, such that the plasma dispersion function can be approximated by the first term from its asymptotic expansion. The dispersion relation then simplifies to [13]

$$1 - \sum_s \sum_{n=1}^{\infty} \frac{2n^2 \omega_{ps}^2}{\omega^2 - n^2 \Omega_{cs}^2} \frac{e^{-\lambda} I_n(\lambda)}{\lambda} = 0. \quad (70)$$

The solutions, which are known as Bernstein modes, are found near each harmonic of the cyclotron frequency of each species. Here the electron Bernstein modes will

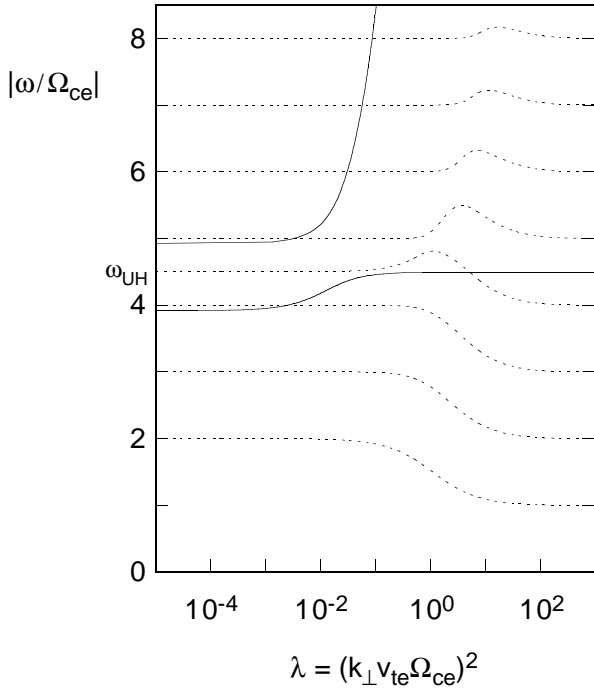


Figure 6: Dispersion relation (70) for electron Bernstein modes (dashed curves). The cold plasma X-mode (full curves) is given for comparison. Parameters are similar to Ref. [14]: $\omega_{UH} = 4.5|\Omega_{ce}|$, $T_e = 1$ keV.

analyzed more closely. In this analysis, the ion contributions can be neglected. For the ion modes one can usually assume $\lambda_e \ll 1$, such that only the $n = 1$ term contributes being well approximated by $\omega_{pe}^2/\Omega_{ce}^2$.

Approximate solutions of the electron Bernstein modes are obtained by assuming $\omega^2 \approx n^2\Omega_{ce}^2$, in the limits $\lambda \ll 1$ and $\lambda \gg 1$. Using Eqs. (30), the dispersion relation becomes

$$\frac{\omega^2 - n^2\Omega_{ce}^2}{n^2\Omega_{ce}^2} \approx \begin{cases} \frac{\omega_{pe}^2(n^2-1)}{(n^2-1)\Omega_{ce}^2 - \omega_{pe}^2} \frac{1}{n!} \left(\frac{\lambda}{2}\right)^{n-1} & \text{for } \lambda \ll 1 \\ \frac{2\omega_{pe}^2}{\Omega_{ce}^2 \lambda \sqrt{2\pi\lambda}} & \text{for } \lambda \gg 1 \end{cases} \quad (71)$$

Note, that in the small λ limit both the contributions from $n = 1$ and the relevant harmonic resonance have been retained, while in the limit of large λ only the harmonic resonance contributes. For $\lambda \ll 1$, one now discerns the cases with $n^2 < \omega_{UH}^2/\Omega_{ce}^2$ for which the right hand side is negative, or $n^2 > \omega_{UH}^2/\Omega_{ce}^2$ for which the right hand side is positive. Here, $\omega_{UH}^2 = \omega_{pe}^2 + \Omega_{ce}^2$ is the Upper Hybrid frequency, where the cold plasma X-mode exhibits a resonance. Further, one observes that for $\lambda \gg 1$ the dispersion curve approaches the cyclotron resonance from above, and that the dispersion curve cannot cross the lines $\omega = n|\Omega_{ce}|$. This leads to the

following picture of the dispersion curves. For $n^2 < \omega_{UH}^2/\Omega_{ce}^2$, the dispersion curve starts at $\omega = n|\Omega_{ce}|$ at $\lambda = 0$ and then drops to $\omega = (n-1)|\Omega_{ce}|$ at $\lambda = \infty$. For $n^2 > \omega_{UH}^2/\Omega_{ce}^2$, the dispersion curve starting at $\omega = n|\Omega_{ce}|$ first increases, and then drops back to $\omega = n|\Omega_{ce}|$ at $\lambda = \infty$. This behaviour of the electron Bernstein modes is illustrated in Fig. 6.

The dispersion of ion Bernstein modes is very similar to that of the electron modes, but slightly more complicated in the presence of multiple ion species. An important role is again plaid by hybrid resonances: solutions of the full dispersion relation show conversion of cold-plasma X-mode waves to Bernstein waves as one of the hybrid resonances is approached. This scheme of mode conversion to Bernstein waves is used in the application of wave in the ion cyclotron range of frequencies [8] and for EC heating of over-dense plasma (Section III.D and [12]).

ACKNOWLEDGMENTS

This work was performed under the Euratom-FOM association agreement with financial support from NWO, and Euratom.

REFERENCES

1. P. Lamalle, Kinetic theory of plasma waves: Part I Introduction, these proceedings.
2. B.D. Fried, S.D. Conte, *The plasma dispersion function*, Academic Press, New York (1961).
3. T.H. Stix, *Waves in plasmas*, AIP, New York (1992).
4. D.G. Swanson, *Plasma Waves*, Academic Press, San Diego (1989).
5. R.A. Cairns, *Radiofrequency Heating of Plasmas*, IOP Publishing, Bristol (1991).
6. J.P. Goedbloed, Introduction to MHD instabilities, these proceedings.
7. R. Koch, The coupling of electromagnetic power to plasmas, these proceedings.
8. R. Koch, Ion cyclotron heating, these proceedings.
9. D.W. Faulconer, Current drive, these proceedings.
10. J.A. Hoekzema, Electron cyclotron heating, these proceedings.
11. J. Preinhaelter, V. Kopecký, J. Plasma Phys. **10**, 1 (1973).
12. H.P. Laqua, et al., Phys. Rev. Lett. **78**, 18 (1997).
13. D.B. Melrose, *Instabilities in space and laboratory plasmas*, Cambridge University Press (1986).
14. S. Puri, F. Leuterer, M. Tutter, J. Plasma Phys. **9**, 89 (1973).